# PART I

# ENABLING TECHNOLOGIES FOR WIRELESS BROADBAND NETWORKS

# CHAPTER 1

# ORTHOGONAL FREQUENCY-DIVISION MULTIPLEXING AND OTHER BLOCK-BASED TRANSMISSIONS

## 1.1 INTRODUCTION

In this chapter we first provide a brief introduction to the basics of wireless communication systems. Then we focus on reviewing various block-based transmission schemes that play important roles in the physical-layer design of wireless broadband networks. These schemes include orthogonal frequency-division multiplexing (OFDM), single-carrier cyclic prefix (SCCP), orthogonal frequency-division multiple access (OFDMA), interleaved frequency-division multiple access (IFDMA), single-carrier frequency-division multiple access (SC-FDMA), cyclic prefix-based code-division multiple access (CP-CDMA), and multicarrier code-division multiple access (MC-CDMA). From these schemes, we also establish a generic input–output model and review linear and nonlinear equalizers that can be used to recover the transmitted signals.

## 1.2 WIRELESS COMMUNICATION SYSTEMS

From a physical-layer perspective, the block diagram of a wireless communication system shown in Figure 1.1 consists of three key components: the transmitter, the wireless channel, and the receiver. On the transmitter side, the design objective is to transform the information bits into a signal format suitable for transmission over

*Wireless Broadband Networks*, By David Tung Chong Wong, Peng-Yong Kong, Ying-Chang Liang, Kee Chaing Chua, and Jon W. Mark

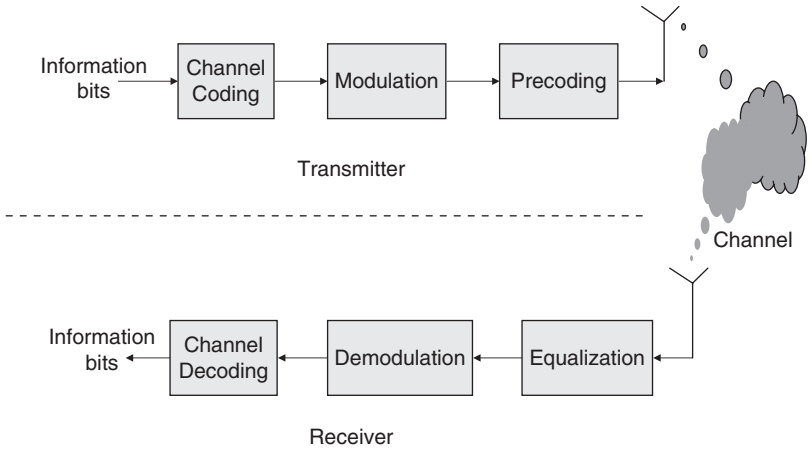


**FIGURE 1.1** Block diagram of a wireless communication system.

the wireless channel. The major elements in the transmitter include channel coding, modulation, and linear or nonlinear precoding.

When the signal passes through the wireless channel, the signal will be attenuated due to propagation loss, shadowing, and multipath fading, and the waveform of the signal received will be different from the one transmitted, due to multipath delay, the time/frequency selectivity of the channel, and the addition of noise and unwanted interference. Finally, at the receiver side, the information bits transmitted are to be recovered through the operations of equalization, demodulation, and channel decoding.

With channel coding, the information bits are converted into coded bits with redundancy so that the effect of channel noise and multipath fading can be minimized. The modulation operation transforms the coded bits into modulated symbols for the purpose of achieving efficient transmission of the signal over the channel with a given bandwidth. The objective of the precoding operation is to provide robustness over the fading channel with multipath delay, or to compensate for the unwanted interference.

The equalization operation estimates the modulated symbols by removing the effect of the channel. Through proper design of the precoding operation, equalization sometimes becomes very simple. The demodulation operation converts the estimated symbols into a bit format, which is then used to recover the information bits through the channel decoding operation.

### 1.2.1 Frequency-Selective Fading Channels

In a wireless propagation environment, the signal transmitted arrives at the receiver with multiple delayed and attenuated versions, and these versions are added up and received by the receiver. The difference in traveling time, $\tau$, between the shortest and longest paths is called *excess delay spread*. When the excess delay spread is much smaller than the symbol period, $T_s$, the channel can be described by a single delay tap. With this single delay tap, in the frequency domain, the channel responses are flat

within the channel bandwidth; thus, the channel is said to be a *flat fading channel*. If the excess delay spread is relatively large compared to the symbol period, the channel can be described by multiple delay taps, and in the frequency domain, the channel responses are no longer flat for all frequencies of interest; thus, this channel is called a *frequency-selective fading channel*.

Suppose that we have a sequence of modulated symbols $\{x(n)\}$ transmitted at the symbol rate of $1/T_s$, through a frequency-selective fading channel. At the receiver, after sampling at the symbol rate, we receive a sequence of received samples $\{y(n)\}$. The relationship between $\{y(n)\}$ and $\{x(n)\}$ is given by

$$y(n) = \sum_l h_l(n)x(n-l) + \tilde{u}(n), \tag{1.1}$$

where $\tilde{u}(n)$ is the additive noise and $h_l(n)$ is the $l$th delay tap of the channel at time $n$.

We can further characterize the channel as a fast fading or slow fading channel, based on the relationship between the bandwidth of the transmitted signal and the Doppler shift of the wireless channel. When the Doppler shift is relatively significant compared to the signal bandwidth, the channel is called a *fast-fading channel* and $h_l(n)$ changes with time $n$; otherwise, the channel is referred to as a *slow-fading channel* and $h_l(n)$ is invariant to the time instant $n$. When slow fading is considered, for description brevity, we drop the time variable in the channel coefficients.

### 1.2.2 Receiver Equalization

It is seen from equation (1.1) that for a frequency-selective fading channel, the signal received at a time instant is the superposition of weighted and delayed versions of the symbols transmitted. This results in introducing *intersymbol interference* (ISI). Let $N$ be the number of transmitted symbols and $L$ be the number of channel taps spaced at a symbol interval; then the receiver collects $N + L - 1$ samples, which are related to the entire number of symbols transmitted. Equalizers have to be designed at the receiver to compensate for ISI and to recover the symbols transmitted.

The optimal equalizer involves maximum likelihood (ML) detection, which requires very high computational complexity. Suboptimal equalizers have thus been proposed which can be implemented in either linear or nonlinear fashion and require complexity much reduced from ML detection. The performance of these suboptimal receivers is, however, usually far away from the performance bound achieved by ML detection.

## 1.3 BLOCK-BASED TRANSMISSIONS

To reduce the computational complexity of equalization, block-based transmissions have been proposed. Specifically, in a *block-based transmission*, the entire sequence of

modulated symbols is first divided into multiple blocks, each is preprocessed further using linear transforms, and guard symbols are inserted between two consecutive blocks. If the length of the guard symbols is longer than the channel memory, two consecutive blocks will not interfere with each other; thus, each block can be equalized separately.

Two types of guard symbols are applicable in block-based transmissions. One is *zero padding*, which inserts zeros between two consecutive blocks; the other is *cyclic prefix* (CP), which is the copy of the last portion of the signal block. In the following, we describe the properties of CP-based block transmissions.

### 1.3.1 Use of a Cyclic Prefix

The block diagram of a CP-based block transmission system is shown in Figure 1.2. Let $N$ be the length of one signal block and denote the signal block to be transmitted through a frequency-selective fading channel as follows:

$$\boldsymbol{x} = [x(0) \quad x(1) \quad \cdots \quad x(N-1)]^T. \tag{1.2}$$

The channel is characterized by a channel impulse response (CIR) $\boldsymbol{h} = [h_0 \quad h_1 \quad \cdots \quad h_{L-1}]^T$, which contains $L$ equally spaced time-domain taps (spaced at symbol intervals $T_s$).

Instead of transmitting block $\boldsymbol{x}$ directly, a new block, $\tilde{\boldsymbol{x}}$, is generated and transmitted through the channel. The new block is formed by appending the last $P$ symbols of $\boldsymbol{x}$ to the head of itself. The portion of the first $P$ symbols in the new block $\tilde{\boldsymbol{x}}$ is the

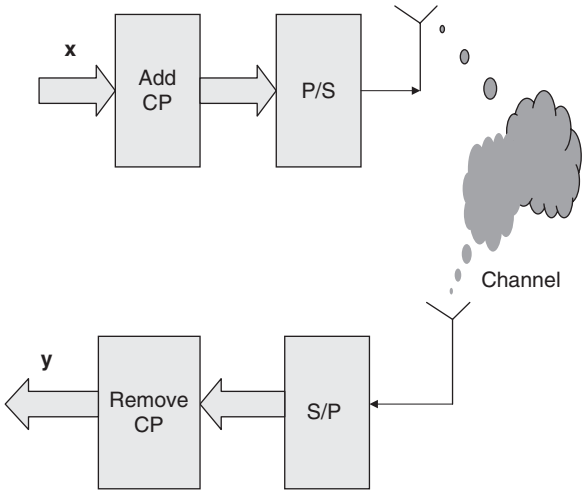


**FIGURE 1.2** Block diagram of a CP-based block transmission system.

cyclic prefix (CP). Then the new block $\tilde{\boldsymbol{x}}$ can be represented by

$$\begin{aligned}\tilde{\boldsymbol{x}} &= [\tilde{x}(0) \ \cdots \ \tilde{x}(P-1) \ \tilde{x}(P) \ \tilde{x}(P+1) \ \tilde{x}(P+2) \ \cdots \ \tilde{x}(P+N-1)]^T \\ &= \Bigg[ x(N-P) \ \cdots \ x(N-1) \ \underbrace{x(0) \ x(1) \ \cdots \ x(N-P) \ \cdots \ x(N-1)}_{x^T} \Bigg]^T .\end{aligned} \tag{1.3}$$

With the transmitted signal $\tilde{\boldsymbol{x}}$, the received signal becomes

$$\tilde{y}(v) = \sum_{l=0}^{L-1} h_l \tilde{x}(v-l) + \tilde{u}(v), \qquad v = 0, 1, \ldots, P+N+L-1, \tag{1.4}$$

where $\tilde{u}(v)$ is additive complex Gaussian random variable with zero mean and variance $E\left\{|\tilde{u}(v)|^2\right\} = N_0$.

The $P$ received signal samples from $\tilde{y}(0)$ to $\tilde{y}(P-1)$ associated with the CP portion are discarded, and we are interested in the received signal samples from $\tilde{y}(P)$ to $\tilde{y}(P+N-1)$, which are associated with the data block. From (1.4), when $P \geq L-1$, we can write the following equations:

$$\begin{aligned}\tilde{y}(P) &= h_0 x(0) + h_1 x(N-1) + \cdots + h_{L-1} x(N-L+1) + \tilde{u}(P), \\ \tilde{y}(P+1) &= h_0 x(1) + h_1 x(0) + \cdots + h_{L-1} x(N-L+2) + \tilde{u}(P+1), \\ &\vdots \\ \tilde{y}(P+N-1) &= h_0 x(N-1) + h_1 x(N-2) + \cdots + h_{L-1} x(N-L) \\ &\quad + \tilde{u}(P+N-1).\end{aligned} \tag{1.5}$$

If we collect the $N$ received signal samples in (1.5) to form a vector $\boldsymbol{y} = [\tilde{y}(P) \quad \tilde{y}(P+1) \quad \cdots \quad \tilde{y}(P+N-1)]^T$, this vector can be written as

$$\boldsymbol{y} = \boldsymbol{H}\boldsymbol{x} + \tilde{\boldsymbol{u}}, \tag{1.6}$$

where $\tilde{\boldsymbol{u}} = [\tilde{u}(P) \quad \tilde{u}(P+1) \quad \cdots \quad \tilde{u}(P+N-1)]^T$, and thanks to the addition of CP, $\boldsymbol{H}$ is now a circular matrix of size $N \times N$ given by

$$\boldsymbol{H} = \begin{bmatrix} h_0 & 0 & \cdots & 0 & h_{L-1} & h_{L-2} & \cdots & h_1 \\ h_1 & h_0 & 0 & \cdots & 0 & h_{L-1} & \cdots & h_2 \\ \vdots & \ddots & \ddots & \ddots & \ddots & \ddots & \ddots & \vdots \\ 0 & \cdots & 0 & h_{L-1} & h_{L-2} & \cdots & h_1 & h_0 \end{bmatrix}. \tag{1.7}$$

Note that what we have developed so far is for the transmission of a single block. To transmit multiple blocks consecutively, Figure 1.3 shows the structure of continuous transmission with CP. From this figure it is clear that some signals received at the beginning of a block are affected by symbols transmitted from the previous block. This

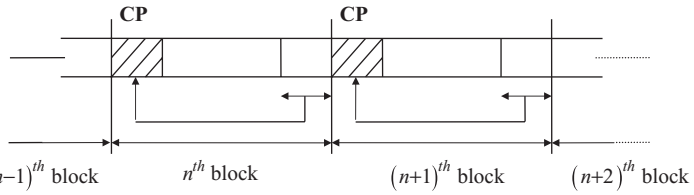


**FIGURE 1.3** Structure of continuous transmission with CP.

phenomenon is called *interblock interference* (IBI). Again, if $P \geq L-1$, inserting CP and discarding the received signals associated with CP help to eliminate the IBI.

### 1.3.2 Relation Between Vectors *x* and *y*

The circular matrix $\boldsymbol{H}$ in (1.7) can be decomposed into the form

$$\boldsymbol{H} = \boldsymbol{W}_N^H \boldsymbol{\Lambda} \boldsymbol{W}_N, \tag{1.8}$$

where:

- $\boldsymbol{W}_N \in \mathbb{C}^{N\times N}$ is the $N \times N$ discrete Fourier transform (DFT) matrix, given by

$$\boldsymbol{W} = \frac{1}{\sqrt{N}} \begin{bmatrix} 1 & 1 & \cdots & 1 \\ 1 & e^{-j2\pi/N} & \cdots & e^{-j2\pi(N-1)/N} \\ \vdots & \ddots & \ddots & \vdots \\ 1 & e^{-j2\pi(N-1)/N} & \cdots & e^{-j2\pi(N-1)(N-1)/N} \end{bmatrix} \tag{1.9}$$

  Note that $\boldsymbol{W}_N^H \boldsymbol{W}_N = \boldsymbol{I}_N$.
- $\boldsymbol{\Lambda} = \text{diag}\{H_0, H_1, \ldots, H_{N-1}\} \in \mathbb{C}^{N\times N}$ is a diagonal matrix with diagonal elements defined by frequency responses, $H_k$, of the channel; that is, $H_k = \sum_{l=0}^{L-1} h_l e^{-j2\pi kl/N}$ for $k = 0, 1, \ldots, N-1$.

The proof of (1.8) is given in the appendix at the end of the chapter. From (1.6) and (1.8), we have the following relation between $\boldsymbol{x}$ and $\boldsymbol{y}$:

$$\boldsymbol{y} = \boldsymbol{W}_N^H \boldsymbol{\Lambda} \boldsymbol{W}_N \boldsymbol{x} + \tilde{\boldsymbol{u}}. \tag{1.10}$$

### 1.3.3 Overview of Block-Based Transmissions

By proper design of the transmitted signal vector $\boldsymbol{x}$ in (1.10), various block-based transmission schemes can be developed, including but not limited to the following:

- Orthogonal frequency-division multiplexing (OFDM) system
- Single-carrier cyclic prefix (SCCP) system
- Orthogonal frequency-division multiple access (OFDMA)

- Interleaved frequency-division multiple access (IFDMA)
- Single-carrier frequency-division multiple access (SC-FDMA)
- Cyclic prefix–based code-division multiple access (CP-CDMA)
- Multicarrier code-division multiple access (MC-CDMA)

OFDMA, IFDMA, SC-FDMA, CP-CDMA, and MC-CDMA are designed to support multiple users to share the same radio resource simultaneously. OFDM and SCCP systems, however, are designed to support single-user communication only. Thus, to support multiple users in sharing the same radio resource, they have to be used in conjunction with other multiple-access schemes, such as time-division multiple access (TDMA) or frequency-division multiple access (FDMA). In TDMA, the time resource is divided into time slots and each user is allowed to use the entire frequency band when it is allocated to use the time slot. In FDMA, the frequency resource is divided into frequency subbands, and each user is allowed to use the entire time resource at the frequency subband allocated to the user. In the following sections, the details of each scheme are provided.

## 1.4 ORTHOGONAL FREQUENCY-DIVISION MULTIPLEXING SYSTEMS

Orthogonal frequency-division multiplexing (OFDM) is a discrete Fourier transform (DFT)–based multicarrier modulation (MCM) scheme [1,2]. The basic idea of OFDM is to transform a frequency-selective fading channel into several parallel frequency flat fading subchannels on which modulated symbols are transmitted. OFDM has been widely adopted in various communications systems, including the digital audio broadcast (DAB) [3] and digital terrestrial video broadcast (DVB-T) [4] standards in Europe and Japan, the IEEE 802.11a/11n wireless local area network (WLAN) [5], and the asymmetric digital subscriber loop (ADSL) [6].

### 1.4.1 System Description

The block diagram of an OFDM system is depicted in Figure 1.4. A sequence of data symbols $\{s(n;v)\}_{v=0}^{N-1}$ is first serial-to-parallel (S/P)-converted to form the $n$th data block $\boldsymbol{s}(n) = [s(n;0) \quad s(n;1) \quad \cdots \quad s(n;N-1)]^T$. This block is transformed by the inverse DFT (IDFT) operation. The output of the IDFT is the transmitted signal block $\boldsymbol{x}(n)$. This block is added with the CP portion as shown in Section 1.2, and the resulting block is parallel-to-serial (P/S)-converted for transmission. The relation between the data block and the transmitted signal block is given by

$$\boldsymbol{x}(n) = \boldsymbol{W}_N^H \boldsymbol{s}(n). \tag{1.11}$$

At the receiver side, the receiver first discards the received signal samples associated with the CP portion. The received signal samples associated with the data block are then fed to the DFT operation. The output of the DFT is passed through the

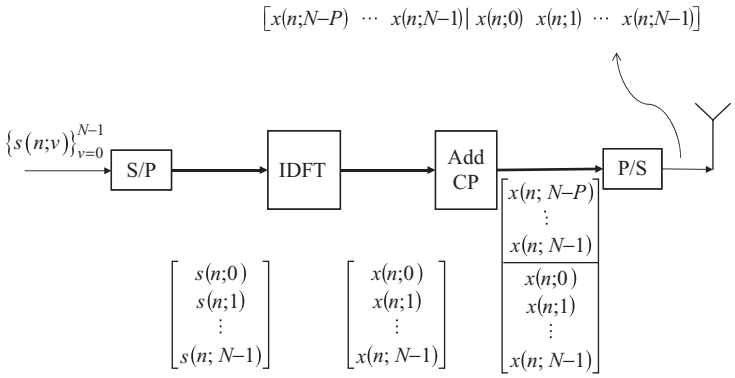


**FIGURE 1.4** Block diagram of an OFDM transmitter.

equalizer to recover the data symbols. These operations are illustrated in Figure 1.5. Based on (1.10) and (1.11), we have

$$\boldsymbol{y}(n) = \boldsymbol{W}_N^H \boldsymbol{\Lambda} \boldsymbol{s}(n) + \tilde{\boldsymbol{u}}(n). \tag{1.12}$$

After the DFT, we obtain

$$\boldsymbol{z}(n) = \boldsymbol{W}_N \, \boldsymbol{y}(n) = \boldsymbol{\Lambda} \boldsymbol{s}(n) + \boldsymbol{u}(n), \tag{1.13}$$

where $\boldsymbol{u} = \boldsymbol{W}_N \tilde{\boldsymbol{u}}$.

It is clear from (1.13) that OFDM transforms a frequency-selective fading channel into a number of frequency flat channels which are called *subchannels*. The output at the $k$th subcarrier is given by

$$z(n;k) = H_k s(n;k) + u(n;k), \qquad k = 0, 1, \ldots, N-1. \tag{1.14}$$

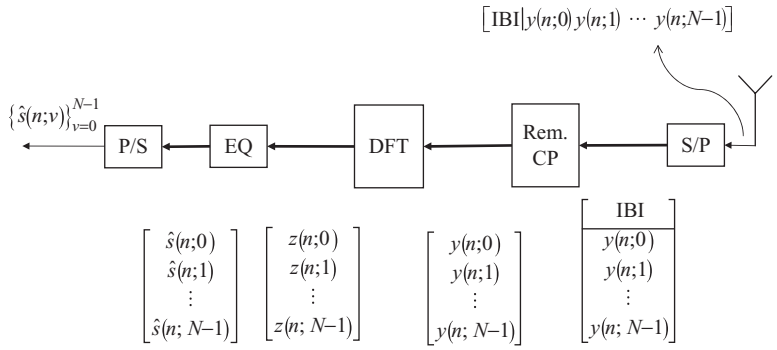


**FIGURE 1.5** Block diagram of an OFDM receiver.

At the receiver, thanks to (1.14), a one-tap equalizer can be applied to each of the subcarrier outputs to recover the transmitted symbol delivered over that subcarrier. More specifically, the coefficient of the zero-forcing (ZF) equalizer is

$$C(n;k)=\frac{1}{H_k}, \qquad k=0,1,\ldots,N-1, \tag{1.15}$$

while that of the minimum mean square error (MMSE) equalizer becomes

$$C(n;k)=\frac{H_k^*}{|H_k|^2+N_0/E_s}, \qquad k=0,1,\ldots,N-1, \tag{1.16}$$

where $E_s$ is the average energy on every modulated symbol. The recovered symbol on the $k$th subcarrier is obtained by rounding

$$\bar{s}(n;k)=C(n;k)z(n;k), \qquad k=0,1,\ldots,N-1, \tag{1.17}$$

to the closest element of the signal constellation in use. This process is also referred to as *slicing*.

### 1.4.2 Advantages and Disadvantages of OFDM Systems

One of the attractive features offered by OFDM is that it provides relatively simple one-tap frequency-domain equalization over the complex time-domain equalization used in conventional single-carrier systems. Furthermore, since OFDM has decoupled the frequency-selective fading channel into a parallel set of flat fading channels over the subcarriers, a more fascinating advantage of OFDM is that it allows power and bit loading over the subcarriers, and by doing so, for a given power budget the channel capacity can be maximized.

OFDM suffers from some drawbacks, however. For example, timing synchronization error results in the IBI. Carrier frequency offset destroys the orthogonality among the subcarriers and introduces intercarrier interference (ICI). The presence of IBI and/or ICI degrade the system's performance dramatically [7, Chap. 2]. Another shortcoming of OFDM is its high peak-to-average power ratio (PAPR). When OFDM signal with high PAPR passes through a nonlinear device, high peak signals may be clipped. The distortions caused by this clipping will affect the orthogonality of subcarriers.

## 1.5 SINGLE-CARRIER CYCLIC PREFIX SYSTEMS [8]

As OFDM suffers from high PAPR, a single-carrier duo of OFDM has been proposed, and this system is called single-carrier cyclic prefix (SCCP) system. The block diagram of a SCCP system is depicted in Figure 1.6. The symbols transmitted are first grouped into blocks. Unlike OFDM, where these blocks are transformed using IDFT

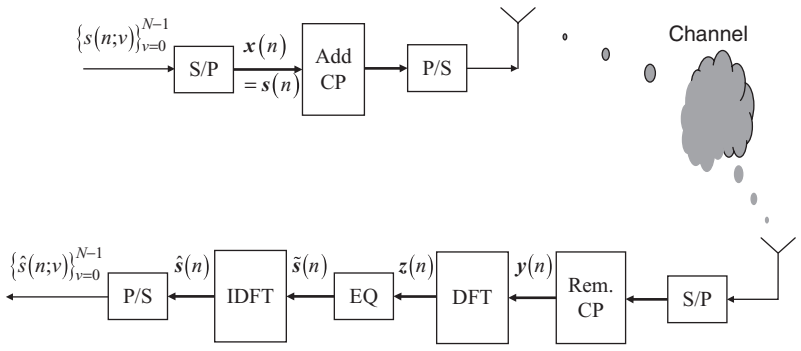


**FIGURE 1.6** Block diagrams of SCCP transmitter and receiver.

before CPs are appended, in SCCP, CPs are inserted directly to these blocks. After that, the resulting blocks are parallel-to-serial-converted and delivered to the transmitting antenna for transmission. At the receiver, the received signal samples associated with the CP portion are removed and the received signal block is transformed to the frequency domain to perform equalization. Finally, the estimated block symbols are transformed back to the time domain for symbol detection.

From Figure 1.6, if we choose $\boldsymbol{x}(n) = \boldsymbol{s}(n)$ and $\boldsymbol{y}(n)$ is filtered as $\boldsymbol{z}(n) = \boldsymbol{W}_N \boldsymbol{y}(n)$, we have

$$\boldsymbol{z}(n) = \boldsymbol{\Lambda} \boldsymbol{W}_N \boldsymbol{s}(n) + \boldsymbol{u}(n). \tag{1.18}$$

Based on (1.18), a frequency-domain equalizer can be deployed to recover the symbols transmitted. More specifically, let $\tilde{\boldsymbol{s}}(n) = \boldsymbol{W}_N \boldsymbol{s}(n)$; then (1.18) reads

$$\boldsymbol{z}(n) = \boldsymbol{\Lambda} \tilde{\boldsymbol{s}}(n) + \boldsymbol{w}(n). \tag{1.19}$$

A ZF or MMSE equalizer can be applied in (1.19) to estimate $\tilde{\boldsymbol{s}}(n)$. After that, the transmitted symbols are recovered as

$$\hat{\boldsymbol{s}}(n) = \boldsymbol{W}_N^H \tilde{\boldsymbol{s}}(n). \tag{1.20}$$

SCCP has been adopted as a part of the IEEE 802.16 standards for wireless metropolitan area networks (WMANs).

## 1.6 ORTHOGONAL FREQUENCY-DIVISION MULTIPLE ACCESS

With the increasing demand on high-data-rate applications and more users supported in a geographical area, orthogonal frequency-division multiple access (OFDMA), which is a combination of OFDM and FDMA, has been proposed to support multiple

users simultaneously. First adopted for cable TV (CATV) networks [9], OFDMA has been used in the uplink of the interaction channel for digital terrestrial television (DVB-RCT) [10] and in the IEEE 802.16 standards for WMAN [11]. OFDMA has also been used in satellite communication [12] and third-generation cellular system long-term evolution (3G-LTE).

### 1.6.1 Subcarrier Allocation

In an OFDMA system, a number of users transmit their information data simultaneously on a number of available subcarriers. Each user is assigned to a set of subcarriers called a *subchannel*. Different subchannels are mutually exclusive. More specifically, suppose that there are $N$ subcarriers and $U$ users in the system. $N$ subcarriers are divided into $S$ subchannels, in which one subchannel consists of $P = N/S$ subcarriers. It is obvious that the system can, at maximum, support only $U \leq S$ users simultaneously.

In a subcarrier assignment scheme [13], each user's subchannel occupies a group of $P$ adjacent subcarriers. This scheme is called *localized subcarrier allocation*. For this scheme, frequency diversity offered by a multipath channel is not obtained because a deep fade can occur over a large number of subcarriers assigned to a given user.

To overcome the drawback of localized subcarrier allocation, distributed subcarrier allocation was proposed [14]. In this scheme, subcarriers belonging to a given user are uniformly distributed over the entire set of $N$ subcarriers. This allocation method reduces the probability that a substantial number of carriers of a user experience a deep fade at the same time. Hence, the frequency diversity can be exploited fully. In a more flexible way, each user can select the best available subcarriers (i.e., those available subcarriers having the highest signal-to-noise ratios for that particular user). By doing so, the sum rate of the system can be maximized.

## 1.7 INTERLEAVED FREQUENCY-DIVISION MULTIPLE ACCESS

Interleaved frequency-division multiple access (IFDMA) is a multiple-access scheme combining the advantages of spread-spectrum and multicarrier transmission. By assigning each user a set of orthogonal subcarriers, no multiple-access interference (MAI) arises even in a severe frequency-selective fading channel. At the receiver side, user discrimination is done using FDMA. Selecting the subcarriers for a particular user from the set of interleaved subcarriers, IFDMA is by nature a single-carrier-based system.

IFDMA has the following advantages over other multiple-access schemes. In comparison with TDMA, IFDMA uses continuous transmission. Compared to CDMA, no MAI is present. With respect to traditional FDMA, IFDMA is capable of achieving better frequency diversity. Moreover, IFDMA overcomes the large power backoff problems associated with its competitor OFDM/OFDMA by reducing the peak/average power ratio, since it employs a single-carrier modulation [16]. The IFDMA symbols transmitted can be generated in two ways, in either the time [15] or the frequency domain [16].

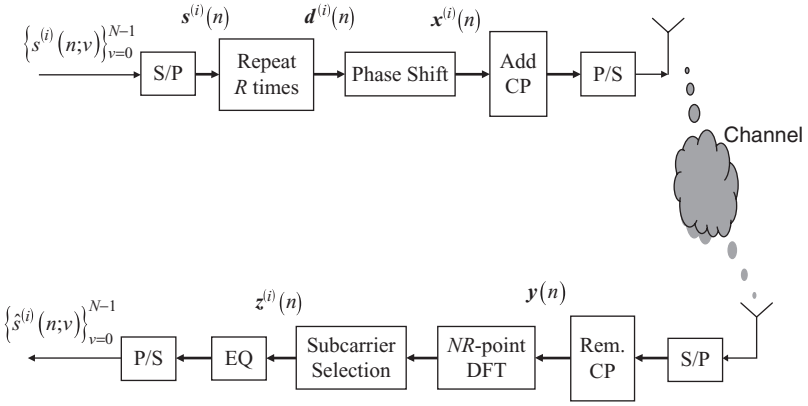


**FIGURE 1.7** Block diagram of an IFDMA system with the transmitter implemented in the time domain.

### 1.7.1 Time-Domain Implementation

Consider a CP-based block transmission scheme in which the $n$th data block of length $N$ belonging to the $i$th user is denoted as

$$s^{(i)}(n) = [s^{(i)}(n;0) \quad s^{(i)}(n;1) \quad \cdots \quad s^{(i)}(n;N-1)]^T.$$

It is obtained from the S/P operation on a data sequence $\{s^{(i)}(n;v)\}_{v=0}^{N-1}$. Denote $R$ as the repetition times, or alternatively, the spreading factor in the frequency-domain implementation, which has to satisfy the condition to avoid overloading the system. The block diagram for time-domain implementation of an IFDMA transmitter is depicted in Figure 1.7.

Next, the $n$th data block is compressed and repeated $R$ times. The resulting $n$th IFDMA symbol is given by

$$\boldsymbol{d}^{(i)}(n) = \frac{1}{\sqrt{R}} \left[ \underbrace{s^{(i)}(n;0) \ \cdots \ s^{(i)}(n;N-1) \ \cdots \ s^{(i)}(n;0) \ \cdots \ s^{(i)}(n;N-1)}_{R \text{ times}} \right]^T. \tag{1.21}$$

This IFDMA symbol for the $i$th user is then modified by a phase vector $\boldsymbol{p}^{(i)}$ of size $NR$ in which the $l$th component is expressed as

$$p^{(i)}(l) = \exp(-jl\varphi^{(i)}), \qquad l = 0, 1, \ldots, NR-1, \tag{1.22}$$

where $\varphi^{(i)} = i(2\pi/NR)$ is the user-dependent phase shift. The elementwise multiplication of $\boldsymbol{d}^{(i)}(n)$ and $\boldsymbol{p}^{(i)}$ assures orthogonality among different users [15]. The

resulting signals for the $i$th user are given as

$$\boldsymbol{x}^{(i)}(n) = \left[d^{(i)}(n;0) \quad d^{(i)}(n;1)e^{-j\varphi^{(i)}} \quad \cdots \quad d^{(i)}(n;NR-1)e^{-j(NR-1)\varphi^{(i)}}\right]^T. \tag{1.23}$$

With the user-dependent phase shift, each user is assigned a set of orthogonal frequencies and such operation facilitates easy user separation at the receiver side. Before transmission, CP is inserted to the front of each block $\boldsymbol{x}^{(i)}(n)$ to eliminate IBI.

Assume that the channel for the $i$th user is a frequency-selective fading channel with $L$ equally spaced time-domain taps, $\boldsymbol{h}^{(i)} = [h_0^{(i)} \quad h_1^{(i)} \quad \cdots \quad h_{L-1}^{(i)}]^T$. The signal samples received from user $i$ after the removal of CP can be written as

$$\boldsymbol{y}^{(i)}(n) = \boldsymbol{W}_{NR}^H \boldsymbol{\Lambda}_{NR}^{(i)} \boldsymbol{W}_{NR} \boldsymbol{x}^{(i)}(n) + \tilde{\boldsymbol{u}}^{(i)}(n), \tag{1.24}$$

where $\boldsymbol{W}_{NR}$ is the $NR \times NR$ DFT matrix, $\boldsymbol{\Lambda}_{NR}^{(i)} = \text{diag}\{\lambda_0^{(i)}, \lambda_1^{(i)}, \ldots, \lambda_{NR-1}^{(i)}\}$, in which $\lambda_k^{(i)} = \sum_{l=0}^{L-1} h_l^{(i)} e^{-j(2\pi/NR)kl}$ denotes the frequency response of the $k$th subcarrier of the channel and $\tilde{\boldsymbol{u}}^{(i)}(n)$ is the addictive noise. At the receiver, the signals received contain signal samples from all users:

$$\boldsymbol{y}(n) = \sum_{i=1}^{U} \boldsymbol{y}^{(i)}(n), \tag{1.25}$$

where $U$ is the total number of users. If we choose

$$U \leq R, \tag{1.26}$$

after $NR$-point DFT, the orthogonality among different users allows us to separate the users by selecting the subcarriers allocated to the $i$th user. The relation between the resulting signal $\boldsymbol{z}^{(i)}(n)$ for the $i$th user with respect to the data block $\boldsymbol{s}^{(i)}(n)$ is given as

$$\boldsymbol{z}^{(i)}(n) = \boldsymbol{\Lambda}_N^{(i)} \boldsymbol{W}_N \boldsymbol{s}^{(i)}(n) + \boldsymbol{u}^{(i)}(n), \tag{1.27}$$

where

$$\boldsymbol{z}^{(i)}(n) = [y^{(i)}(n;i) \quad y^{(i)}(n;i+R) \quad \cdots \quad y^{(i)}(n;i+(N-1)R)]^T$$

and $\boldsymbol{\Lambda}_N^{(i)} = \text{diag}\{\lambda_i^{(i)}, \lambda_{i+R}^{(i)}, \ldots, \lambda_{i+(N-1)R}^{(i)}\}$, and $\boldsymbol{u}^{(i)}$ is a column vector containing the elements of $\tilde{\boldsymbol{u}}^{(i)}$ at positions $\{i, i+R, \ldots, i+(N-1)R\}$. Equation (1.27) is the same as the SCCP model given in (1.18). Thus, although no MAI is present for IFDMA system, intersymbol interference still exists. Various equalization techniques have to be employed to recover the signals transmitted.

### 1.7.2 Frequency-Domain Implementation

Equivalently, the IFDMA transmission signal can be constructed in the frequency domain as illustrated in Figure 1.8. First, $N$-point DFT is performed on each data block $\boldsymbol{s}^{(i)}(n)$. Then the frequency-domain symbols $\boldsymbol{b}^{(i)}(n) = \boldsymbol{W}_N \boldsymbol{s}^{(i)}(n)$ are interleaved in such a way that each user occupies an orthogonal set of subcarriers and the resulting expression of the $k$th subcarrier ($k = 0, 1, \ldots, NR - 1$) from the $i$th user is given as

$$c^{(i)}(n;k) = \begin{cases} b^{(i)}(n;k), & k = k'R + i \qquad (k' = 0, 1, \ldots, N-1) \\ 0, & \text{otherwise,} \end{cases} \tag{1.28}$$

where $R$ represents the frequency spacing between adjacent subcarriers (sometimes called the *spreading factor*) [16]. Finally, the time-domain symbols $\boldsymbol{x}^{(i)}(n)$ obtained after $NR$-point IDFT is inserted with a CP portion before transmission. The resulting transmitted signal implemented in the frequency domain is exactly the same as the one generated in the time domain. Hence, the receiver structure and analysis remain the same as in the previous case.

## 1.8 SINGLE-CARRIER FREQUENCY-DIVISION MULTIPLE ACCESS

For IFDMA, each user is allocated with interleaved subcarriers; thus, frequency diversity can be achieved for all users. The frequency-domain implementation structure of IFDMA provides other ways to allocate subcarriers to the users. For example, in Figure 1.8, each user can be allocated a different set of $N$ consecutive subcarriers, called *localized subcarrier allocation*. With localized subcarrier allocation, the system is called *single-carrier frequency-division multiple access* (SC-FDMA) [17, 18]. Similar to OFDMA systems, SC-FDMA can achieve multiuser diversity.

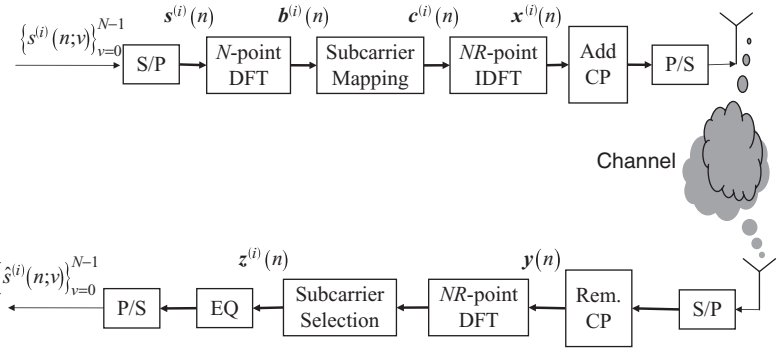


**FIGURE 1.8** Block diagram of an IFDMA system with the transmitter implemented in the frequency domain.

## 1.9 CP-BASED CODE DIVISION MULTIPLE ACCESS

In this section we review CDMA-based block transmissions. In particular, we consider CP-CDMA and MC-CDMA systems. We assume that there are $U$ active users in both systems. Each user has the same processing gain of $G$. The short code for the $i$th user is denoted as $\boldsymbol{c}_i$, where $\boldsymbol{c}_i = [c_i(0) \quad c_i(1) \quad \cdots \quad c_i(G-1)]^T$. All $U$ short codes make up a set of $U$ orthonormal basis vectors (i.e., $\boldsymbol{c}_i^H \boldsymbol{c}_j = 1$ for $i = j$ and $\boldsymbol{c}_i^H \boldsymbol{c}_j = 0$ for $i \neq j$). The long scrambing code for the $n$th data block is denoted by the diagonal matrix $\boldsymbol{D}(n)$.

### 1.9.1 CP-CDMA [19]

In a CP-CDMA system, each user transmits $Q = N/G$ symbols in one data block where $N$ is the size of the data block. The $Q$ symbols of one user are first spread out with the user's specific spreading code. After that, all the chip sequences of all users are added up. The total chip sequence, which has the length of $N$, is then passed through the CP inserter. At the receiver, the received signal samples associated with the CP portion are removed, and then the DFT transform is performed on the remaining signals associated with the data block.

We have the following equation to model the CP-CDMA system:

$$\boldsymbol{z}(n) = \boldsymbol{\Lambda W D}(n)\boldsymbol{C s}(n) + \boldsymbol{w}(n), \tag{1.29}$$

where:

- $\boldsymbol{s}(n) = [\bar{\boldsymbol{s}}_1^T(n) \;\; \bar{\boldsymbol{s}}_2^T(n) \;\; \cdots \;\; \bar{\boldsymbol{s}}_Q^T(n)]^T$; $\bar{\boldsymbol{s}}_v(n) = [s_1(n;v) \;\; s_2(n;v) \;\; \cdots \;\; s_T(n;v)]^T$ for $v = 1, 2, \ldots, Q$, and $s_i(n;v)$ is the $v$th symbol of the $i$th user transmitted on the $n$th data block.
- $\boldsymbol{C} = \text{diag}\left\{\underbrace{\bar{\boldsymbol{C}}, \ldots, \bar{\boldsymbol{C}}}_{Q \text{ times}}\right\}$; $\bar{\boldsymbol{C}} = [\boldsymbol{c}_1 \quad \boldsymbol{c}_2 \quad \cdots \quad \boldsymbol{c}_U]$.

### 1.9.2 MC-CDMA [20]

In an MC-CDMA system, each of the $Q$ symbols from a user is spread in the frequency domain on some subcarriers. The total number of subcarriers in the system is $N = GQ$. On the receiver side, the $n$th block received after DFT can be written as

$$\boldsymbol{z}(n) = \boldsymbol{\Lambda\Pi D}(n)\boldsymbol{C}\,\boldsymbol{s}(n) + \boldsymbol{w}(n), \tag{1.30}$$

where $\boldsymbol{z}(n)$, $\boldsymbol{C}$, $\boldsymbol{s}(n)$, and $\boldsymbol{w}(n)$ are defined as in the CP-CDMA system. The matrix $\boldsymbol{\Pi}$ is the interleaver matrix, which is used to allocate to nonconsecutive subcarriers chips belonging to a symbol.

## 1.10 RECEIVER DESIGN

The fundamental objective of the receiver design in communication systems is to recover the information bits dedicated to a particular receiver. From the derivations above for various multiple-access schemes, we arrive at the following generic input–output model:

$$\boldsymbol{z}(n) = \boldsymbol{H}\boldsymbol{s}(n) + \boldsymbol{u}(n), \tag{1.31}$$

where the channel matrix depends on the specific scheme of interest.

To describe the linear receivers, we make the following assumptions:

- $\boldsymbol{s}(n) = [s(n;1) \quad s(n;2) \quad \cdots \quad s(n;K-1)]^T$ is the signal vector transmitted. We assume that the symbols transmitted, $s(n;k)$' $s$, are zero mean, independent, identically distributed (i.i.d.) with power $E\{|s(n;k)|^2\} = E_S$.
- $\boldsymbol{u}(n) \in \mathbb{C}^{N\times 1}$ is the noise vector, which is assumed to be a zero-mean complex Gaussian random vector with a covariance matrix of $E\{\boldsymbol{u}(n)\boldsymbol{u}^H(n)\} = N_0\boldsymbol{I}_N$.
- The symbols transmitted are statistically independent of the noises.

To facilitate subsequent derivations, we define the signal-to-noise ratio (SNR) as $\Gamma = E_S/N_0$. Our objective is to recover the transmitted signal vector $\boldsymbol{s}(n)$ based on the received signal vector $\boldsymbol{z}(n)$. The ML estimate of $\boldsymbol{s}(n)$ is given by

$$\breve{\boldsymbol{s}}_{\mathrm{ML}}(n) = \arg \min_{\boldsymbol{s}(n)\in C^K} \|\boldsymbol{z}(n) - \boldsymbol{H}\boldsymbol{s}(n)\|^2, \tag{1.32}$$

where $C = \{c_0 \quad c_1 \quad \cdots \quad c_{|C|-1}\}$ is the set containing all constellation points of the modulation scheme in use and $|C|$ is the size of the constellation. Equation (1.32) requires an exhaustive search of all $|C|^K$ possible vectors to find the ML estimate of $\boldsymbol{s}(n)$. This number should be very large when we use higher modulation schemes and/or when the signal dimension $K$ is large. Hence, the ML receiver involves an exponential complexity, and low-complexity suboptimal receivers are desired in practical systems.

In this section we give an overview of two types of suboptimal receivers: linear and nonlinear. Among the linear receivers, zero-forcing and minimum mean square error receivers are chosen due to their simplicity and popularity. However, these receivers provide performance that is far from that of the ML receiver. Hence, nonlinear receivers are also reviewed. We cover the MMSE receiver with soft interference cancellation and a block-iterative generalized decision feedback equalizer.

### 1.10.1 Linear Receivers

The model of linear receivers is represented by matrix $\boldsymbol{C}^H$ in Figure 1.9, where $\boldsymbol{C} = [\boldsymbol{c}_0 \quad \boldsymbol{c}_1 \quad \cdots \quad \boldsymbol{c}_{K-1}]$. A linear receiver uses a weighting vector $\boldsymbol{c}_k$ of dimension $N \times 1$ to decode the $k$th symbol, $s(n;k)$, based on the received signal vector. More

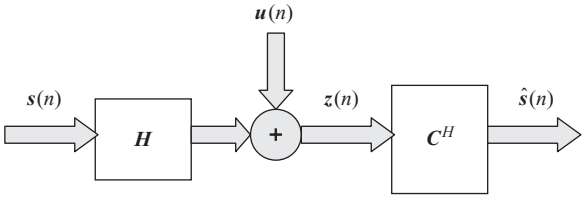


**FIGURE 1.9** Block diagram of linear receivers.

specifically, we calculate the quantity

$$\breve{s}(n;k) = \boldsymbol{c}_k^H \boldsymbol{z}(n) = \boldsymbol{c}_k^H \boldsymbol{h}_k s(n;k) + \sum_{i \neq k} \boldsymbol{c}_k^H \boldsymbol{h}_i s(n;i) + \boldsymbol{c}_k^H \boldsymbol{u}(n). \tag{1.33}$$

The signal component in $\breve{s}(n;k)$ is $\boldsymbol{c}_k^H \boldsymbol{h}_k s(n;k)$, and its power is given by

$$P_S = \left| \boldsymbol{c}_k^H \boldsymbol{h}_k \right|^2 E_S. \tag{1.34}$$

The interference-plus-noise component is $\sum_{i \neq k} \boldsymbol{c}_k^H \boldsymbol{h}_i s(n;i) + \boldsymbol{c}_k^H \boldsymbol{u}(n)$, and its variance is determined by

$$\sigma_k^2 = \sum_{i \neq k} \left| \boldsymbol{c}_k^H \boldsymbol{h}_i \right|^2 E_S + \| \boldsymbol{c}_k \|^2 N_0. \tag{1.35}$$

Hence, the signal-to-interference-plus-noise ratio (SINR) for determining the symbol $s(n;k)$ is given by

$$\mathrm{SINR}_k = \frac{\left| \boldsymbol{c}_k^H \boldsymbol{h}_k \right|^2}{\sum_{i \neq k} \left| \boldsymbol{c}_k^H \boldsymbol{h}_i \right|^2 + (1/\Gamma) \| \boldsymbol{c}_k \|^2 N_0}. \tag{1.36}$$

***1.10.1.1 ZF Receiver*** For the ZF receiver, $\boldsymbol{C}_{\mathrm{ZF}}^H$ is determined by the Moore–Penrose pseudoinverse of $\boldsymbol{H}$. When $\boldsymbol{H}$ is a square matrix and is invertible, $\boldsymbol{C}_{\mathrm{ZF}}^H$ reduces to $\boldsymbol{H}^{-1}$. When $N \geq K$, the Moore–Penrose pseudoinverse of $\boldsymbol{H}$ becomes [21]

$$\boldsymbol{C}_{\mathrm{ZF}}^H = (\boldsymbol{H}^H \boldsymbol{H})^{-1} \boldsymbol{H}^H. \tag{1.37}$$

In this case, the output of the ZF receiver is given by

$$\begin{aligned} \breve{\boldsymbol{s}}(n) &= (\boldsymbol{H}^H \boldsymbol{H})^{-1} \boldsymbol{H}^H (\boldsymbol{H} \boldsymbol{s}(n) + \boldsymbol{w}(n)) \\ &= \boldsymbol{s}(n) + (\boldsymbol{H}^H \boldsymbol{H})^{-1} \boldsymbol{H}^H \boldsymbol{w}(n). \end{aligned} \tag{1.38}$$

It is observed that the ZF receiver tries to null out the interferences from other symbols, and it usually suffers from noise enhancement because of the nulling purpose.

***1.10.1.2 MMSE Receiver*** The MMSE receiver is the optimal linear receiver that maximizes the SINR at the equalization output. To derive this receiver, we define the mean square error (MSE) between the transmitted symbol $s(n;k)$ and the equalization output $\breve{s}(n;k)$ as follows:

$$\begin{aligned} J(\boldsymbol{c}_k) &= E\left\{\left|s(n;k) - \boldsymbol{c}_k^H \boldsymbol{z}(n)\right|^2\right\} \\ &= E\left\{\left|s(n;k)\right|^2\right\} - \boldsymbol{r}_k^H \boldsymbol{c}_k - \boldsymbol{c}_k^H \boldsymbol{r}_k + \boldsymbol{c}_k^H \boldsymbol{R}_z \boldsymbol{c}_k, \end{aligned} \tag{1.39}$$

where $\boldsymbol{R}_z = E\{\boldsymbol{z}(n)\boldsymbol{z}^H(n)\}$ and $\boldsymbol{r}_k = E\{\boldsymbol{z}(n)s^*(n;k)\}$. Differentiating (1.39) with respect to $\boldsymbol{c}_k^*$ [22, App. B], we obtain

$$\frac{\partial J(\boldsymbol{c}_k)}{\partial \boldsymbol{c}_k^*} = \boldsymbol{R}_z \boldsymbol{c}_k - \boldsymbol{r}_k. \tag{1.40}$$

Letting $\partial J(\boldsymbol{c}_k)/\partial \boldsymbol{c}_k^* = \boldsymbol{0}$ yields

$$\boldsymbol{c}_k = \boldsymbol{R}_z^{-1} \boldsymbol{r}_k. \tag{1.41}$$

From (1.31) we have

$$\boldsymbol{R}_z = E\left\{\boldsymbol{z}(n)\boldsymbol{z}^H(n)\right\} = \boldsymbol{H}\boldsymbol{H}^H E_S + N_0 \boldsymbol{I}_N \tag{1.42}$$

and

$$\boldsymbol{r}_k = E\{\boldsymbol{z}(n)s^*(n;k)\} = \boldsymbol{h}_k E_S. \tag{1.43}$$

Therefore, (1.41) can be written as

$$\boldsymbol{c}_k = (\boldsymbol{H}\boldsymbol{H}^H + (1/\Gamma)\boldsymbol{I}_N)^{-1}\boldsymbol{h}_k = \left(\boldsymbol{h}_k \boldsymbol{h}_k^H + \sum_{i \neq k} \boldsymbol{h}_i \boldsymbol{h}_i^H + (1/\Gamma)\boldsymbol{I}_N\right)^{-1} \boldsymbol{h}_k. \tag{1.44}$$

Equivalently, the MMSE receiver for all symbols transmitted can be represented as

$$\boldsymbol{C}_{\text{MMSE}} = (\boldsymbol{H}\boldsymbol{H}^H + (1/\Gamma)\boldsymbol{I}_N)^{-1}\boldsymbol{H}. \tag{1.45}$$

Some parameters of the MMSE receiver that we are interested in are:

- The output SINR for the symbol $s(n;k)$: The generic SINR formula in (1.36) can be written as

$$\text{SINR}_k = \frac{\left|\boldsymbol{c}_k^H \boldsymbol{h}_k\right|^2}{\boldsymbol{c}_k^H \left(\boldsymbol{H}_k \boldsymbol{H}_k^H + (1/\Gamma)\boldsymbol{I}_N\right)\boldsymbol{c}_k}, \tag{1.46}$$

  where $\boldsymbol{H}_k$ is the matrix $\boldsymbol{H}$ in which the $k$th column is removed. Using the matrix inversion lemma† with $\boldsymbol{A} = \boldsymbol{H}_k \boldsymbol{H}_k^H + (1/\Gamma)\boldsymbol{I}_N$, $\boldsymbol{B} = \boldsymbol{h}_k$, $\boldsymbol{C} = \boldsymbol{h}_k^H$, and $\boldsymbol{D} = -1$, we have

$$\left(\boldsymbol{H}\boldsymbol{H}^H + (1/\Gamma)\boldsymbol{I}_N\right)^{-1} = \boldsymbol{A}^{-1} - \frac{\boldsymbol{A}^{-1}\boldsymbol{h}_k \boldsymbol{h}_k^H \boldsymbol{A}^{-1}}{1 + \boldsymbol{h}_k^H \boldsymbol{A}^{-1} \boldsymbol{h}_k}. \tag{1.47}$$

  Thus, the MMSE weight vector $\boldsymbol{c}_k$ in (1.44) is given by

$$\begin{aligned} \boldsymbol{c}_k &= \left(\boldsymbol{H}\boldsymbol{H}^H + (1/\Gamma)\boldsymbol{I}_N\right)^{-1} \boldsymbol{h}_k \\ &= \frac{1}{1 + \boldsymbol{h}_k^H \boldsymbol{A}^{-1} \boldsymbol{h}_k} \boldsymbol{A}^{-1} \boldsymbol{h}_k = \frac{1}{1+\beta_k} \boldsymbol{A}^{-1} \boldsymbol{h}_k, \end{aligned} \tag{1.48}$$

  where $\beta_k = 1 + \boldsymbol{h}_k^H \boldsymbol{A}^{-1} \boldsymbol{h}_k$. Substituting (1.48) in (1.46), we obtain

$$\text{SINR}_k = \beta_k = \boldsymbol{h}_k^H \left(\boldsymbol{H}_k \boldsymbol{H}_k^H + (1/\Gamma)\boldsymbol{I}_N\right)^{-1} \boldsymbol{h}_k. \tag{1.49}$$

- If we define $\alpha_k = \boldsymbol{c}_k^H \boldsymbol{h}_k$, we can easily obtain

$$\alpha_k = \frac{\beta_k}{1+\beta_k}. \tag{1.50}$$

- After placing (1.48) in the general form of variance of interference plus noise in (1.35), we obtain

$$\sigma_k^2 = \boldsymbol{c}_k^H \left(\boldsymbol{H}_k \boldsymbol{H}_k^H E_s + N_0 \boldsymbol{I}_N\right) \boldsymbol{c}_k = \frac{\beta_k}{(1+\beta_k)^2}. \tag{1.51}$$

In the MMSE receiver, for a given $s(n;k)$, when the signal dimension $K$ becomes large, the interference plus noise can be modeled as a zero-mean complex Gaussian random variable. From (1.33) we have

$$E\{\breve{s}(n;k)\} = \alpha_k s(n;k) \neq s(n;k). \tag{1.52}$$

†$(\boldsymbol{A} - \boldsymbol{B}\boldsymbol{D}^{-1}\boldsymbol{C}) = \boldsymbol{A}^{-1} + \boldsymbol{A}^{-1}\boldsymbol{B}(\boldsymbol{D} - \boldsymbol{C}\boldsymbol{A}^{-1}\boldsymbol{B})^{-1}\boldsymbol{C}\boldsymbol{A}^{-1}$ [23].

This result implies that the MMSE receiver produces a biased estimate of $s(n;k)$. For phase-shift-keying (PSK) modulation, if hard decisions are made on $\breve{s}(n;k)$, the BER performance will not be affected by this biased estimate. However, for quadrature amplitude modulation (QAM), this bias does affect the BER performance. Therefore, we need to obtain an unbiased estimate of $s(n;k)$. We can achieve this estimate by multiplying $\breve{s}(n;k)$ with a scaling factor of $1/\alpha_k$, which yields

$$\widehat{s}(n;k) = \frac{1}{\alpha_k}\breve{s}(n;k). \tag{1.53}$$

It is easy to see that $E\{\widehat{s}(n;k)\} = s(n;k)$; hence, $\widehat{s}(n;k)$ is called an *unbiased estimate* of $s(n;k)$.

### 1.10.2 Iterative Receivers

In the preceding section, we studied linear equalizers. In this section, two nonlinear iterative receivers, MMSE-SIC and BI-GDFE, are presented. These receivers have near-ML performance and much reduced complexity.

***1.10.2.1 MMSE-SIC [24]*** We first present the MMSE-SIC receiver to estimate the transmitted symbols in (1.31). Let $\boldsymbol{c}_{k,l}$ be the MMSE weighting vector for the $k$th symbol $s(n;k)$ at the $l$th iteration. At the first iteration, the conventional MMSE is used. Hence, from (1.44), $\boldsymbol{c}_{k,1}$ is determined as

$$\boldsymbol{c}_{k,1} = \left(\boldsymbol{h}_k\boldsymbol{h}_k^H + \sum_{i\neq k}\boldsymbol{h}_i\boldsymbol{h}_i^H + (1/\Gamma)\boldsymbol{I}_N\right)^{-1}\boldsymbol{h}_k. \tag{1.54}$$

From (1.53), the unbiased output of this MMSE receiver for the $k$th symbol is written as

$$\widehat{s}_1(n;k) = \frac{1}{\alpha_{k,1}}\boldsymbol{c}_{k,1}^H\boldsymbol{z}(n) = s(n;k) + r_1(n;k), \tag{1.55}$$

where $\alpha_{k,1} = \boldsymbol{c}_{k,1}^H\boldsymbol{h}_k$ and $r_1(n;k)$ is the residual interference and noise after the bias removal, which is given by

$$r_1(n;k) = \frac{1}{\alpha_{k,1}}\left(\sum_{i\neq k}\boldsymbol{c}_{k,1}^H\boldsymbol{h}_i + \boldsymbol{c}_{k,1}^H\boldsymbol{u}(n)\right). \tag{1.56}$$

With the help of (1.51), we can derive the variance of $r_1(n;k)$ as

$$\sigma_{k,1}^2 = \frac{\boldsymbol{c}_{k,1}^H\left(\boldsymbol{H}_k\boldsymbol{H}_k^H E_s + N_0\boldsymbol{I}_N\right)\boldsymbol{c}_{k,1}}{|\alpha_{k,1}|^2}. \tag{1.57}$$

Hence, the SINR of the output of the $k$th symbol can easily be obtained:

$$\mathrm{SINR}_{k,1} = \frac{\left|\boldsymbol{c}_{k,1}^H \boldsymbol{h}_k\right|^2}{\boldsymbol{c}_{k,1}^H \left(\boldsymbol{H}_k \boldsymbol{H}_k^H + (1/\Gamma)\boldsymbol{I}_N\right) \boldsymbol{c}_{k,1}}. \tag{1.58}$$

The soft estimate of $s(n;k)$ is then calculated as

$$\tilde{s}_1(n;k) = E\left\{s(n;k)|\widehat{s}_1(n;k)\right\} = \frac{\sum_{v=0}^{|C|-1} c_v f(\widehat{s}_1(n;k)|s(n;k)=c_v)}{\sum_{v=0}^{|C|-1} f(\widehat{s}_1(n;k)|s(n;k)=c_v)}, \tag{1.59}$$

where $f(a|b)$ is the probability density function of $a$ given $b$. When the signal dimension $K$ becomes large, the residual $r_1(n;k)$ can be modeled approximately as a zero-mean complex Gaussian random variable with variance of $\sigma_{k,1}^2$; hence,

$$f(\widehat{s}_1(n;k)|s(n;k)=c_v) = \frac{1}{\sqrt{2\pi}\,\sigma_{k,1}^2} \exp\left\{-\frac{|\widehat{s}_1(n;k)-c_v|^2}{2\sigma_{k,1}^2}\right\}. \tag{1.60}$$

Repeating those calculations for $k=0, 1, \ldots, K-1$, we obtain the soft information for all symbols after the first iteration. Suppose that we have the soft information for all symbols after the $l$th iteration. At the $(l+1)$th iteration, for the $k$th symbol, the MMSE-SIC receiver performs soft cancellation of the interference to produce $\boldsymbol{z}_{k,l+1}(n)$ to estimate $s(n;k)$ at the $(l+1)$th iteration as

$$\begin{aligned}\boldsymbol{z}_{k,l+1}(n) &= \boldsymbol{z}(n) - \sum_{i\neq k} \boldsymbol{h}_i \tilde{s}_l(n;i) \\ &= \boldsymbol{h}_k s(n;k) - \sum_{i\neq k} \boldsymbol{h}_i (s(n;i) - \tilde{s}_l(n;i)) + \boldsymbol{u}(n).\end{aligned} \tag{1.61}$$

Based on (1.61), a new MMSE weighting vector, $\boldsymbol{c}_{k,l+1}$, is obtained for the $k$th symbol as follows:

$$\boldsymbol{c}_{k,l+1} = \left(\boldsymbol{h}_k \boldsymbol{h}_k^H + \boldsymbol{H}_k \boldsymbol{D}_{k,l} \boldsymbol{H}_k^H + (1/\Gamma)\boldsymbol{I}_N\right)^{-1} \boldsymbol{h}_k, \tag{1.62}$$

where $\boldsymbol{D}_{k,l} = \mathrm{diag}\{d_{0,l} \quad \cdots \quad d_{k-1,l} \quad d_{k+1,l} \quad \cdots \quad d_{k-1,l}\}$ with

$$\begin{aligned}d_{i,k} &= E\{|s(n;i) - \tilde{s}_l(n;i)|^2 \left|\widehat{s}_l(n;l)\right.\} \\ &= \frac{1}{E_s}(E\{|s(n;i)|^2 \left|\widehat{s}_l(n;i)\right.\} - |\tilde{s}_l(n;i)|^2)\end{aligned} \tag{1.63}$$

and

$$E\{|s(n;i)|^2 \Big| \widehat{s}(n;i).\} = \sum_{v=0}^{|C|-1} |c_v|^2 p(s(n;i) = c_v \Big| \widehat{s}_l(n;i)). \tag{1.64}$$

From the new weighting vector in (1.62) and (1.55), the new unbiased output of the $k$th symbol is determined. Hence, soft interference cancellation is carried out for every iteration. Note that the weighting vectors are different from one symbol interval to another; thus, the computational complexity for MMSE-SIC is still very high.

***1.10.2.2 BI-GDFE [25]*** The block diagram of a BI-GDFE receiver is given in Figure 1.10. This receiver is an iterative receiver in which the decisions obtained from the previous iteration are used to reconstruct the ISI, which is then canceled out from the received signal vector for the purpose of improving the detection performance in later iterations. At the $l$th iteration, the received signal vector $\boldsymbol{z}(n)$ is passed through the feed forward equalizer (FFE) $\boldsymbol{K}_l$. At the same time, the hard decisions from the previous iteration $\hat{\boldsymbol{s}}_{l-1}(n)$ are filtered by the feed-backward equalizer (FBE) $\boldsymbol{D}_l$. The output from the FFE then subtracts the output from the FBE to generate $\hat{\boldsymbol{z}}_l(n)$, which is exploited further to obtain the hard decision $\hat{\boldsymbol{s}}_l(n)$.

The optimal values of $\boldsymbol{K}_l$ and $\boldsymbol{D}_l$ that maximize the SINR at the $l$th iteration are given by [25]

$$\boldsymbol{K}_l = \left[\left(1 - \rho_{l-1}^2\right) \boldsymbol{H}\boldsymbol{H}^H + (1/\Gamma)\boldsymbol{I}_N\right]^{-1} \boldsymbol{H} \tag{1.65}$$

and

$$\boldsymbol{D}_l = \rho_{l-1} \left(\boldsymbol{K}_l^H \boldsymbol{H} - \boldsymbol{A}_l\right), \tag{1.66}$$

where $\boldsymbol{A}_l$ is a diagonal matrix whose diagonal elements are equal to those of $\boldsymbol{K}_l^H \boldsymbol{H}$; $\rho_{l-1}$ is a coefficient that indicates the statistical reliability between the hard decision $\hat{\boldsymbol{s}}_{l-1}(n)$ and the transmitted signal vector $\boldsymbol{s}(n)$, and $E\{\boldsymbol{s}(n)\hat{\boldsymbol{s}}_l^H(n)\} = \rho_{l-1} E_s \boldsymbol{I}_K$.

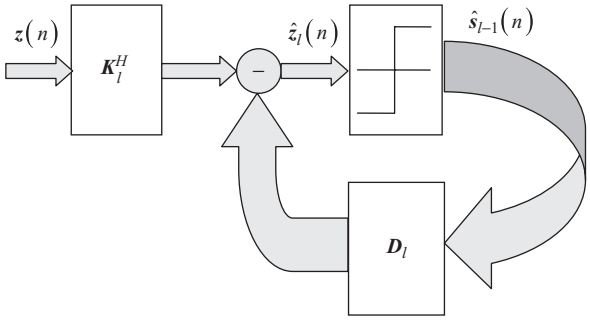


**FIGURE 1.10** Block diagram of a BI-GDFE receiver.

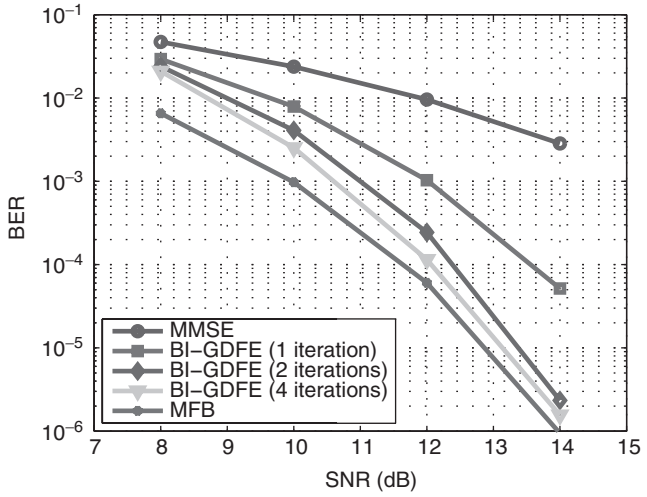


**FIGURE 1.11** Performance of MMSE and BI-GDFE receivers for IFDMA.

Methods for determining the statistical reliability coefficients are studied in [25] for QPSK modulation and in [26] for high-order QAM.

For the first iteration, $\rho_0$ is chosen to be zero and thus the BI-GEFE receiver functions as the conventional MMSE receiver. If the channel matrix $\boldsymbol{H}$ is static over some symbol intervals (block fading channel), the values of $\boldsymbol{K}_l$ and $\boldsymbol{D}_l$ need to be determined once and can be applied to the entire block. This helps to reduce the complexity of a BI-GDFE receiver compared to a MMSE-SIC receiver.

In [25], computer simulations have shown that the BI-GDFE receiver is capable of achieving the single-user matched-filter bound (MFB) for spatial multiplexing based on large random multiple-input, multiple-output (MIMO) channels when the received SNR is high enough. That is, the BI-GDFE receiver is very effective in suppressing the interference between the data streams for MIMO systems.

The use of BI-GDFE in CP-CDMA and MC-CDMA can also be found [27,28], while a reconfigurable BI-GDFE has been proposed [29] for various CP-based block transmissions. As an example, in Figure 1.11 we plot the performance curves of MMSE and BI-GDFE receivers for IFDMA systems with 256 subcarriers, each user being allocated 64 subcarriers and with a channel length of 64. Here, for IFDMA, discontinuous subcarrier mapping is used. From the simulation results it is clear that a BI-GDFE outperforms an MMSE and can achieve a performance close to that of an MFB.

## SUMMARY

Multiple-access schemes play important roles in designing the physical-layer air interfaces of broadband wireless networks. In this chapter, various multiple-access

schemes have been reviewed in detail from transmitter and receiver perspectives. We have also reviewed linear and nonlinear equalizers for generic transmission models. Recommendations for further reading are as follows:

- Equivalence and relationship of MMSE-SIC and BI-GDFE [26]
- Resource allocation for multiuser OFDM systems [30–32]
- Resource allocation for OFDMA [33]

## APPENDIX: PROOF OF (1.8)

We first prove the following theorem.

**Theorem 1.1** Consider the following two sequences:

- *Sequence 1:* $[x(0) \quad x(1) \quad \cdots \quad x(N-1)]$.
- *Sequence 2:* $[\tilde{x}(0) \quad \tilde{x}(1) \quad \cdots \quad \tilde{x}(N-1)]$.

Their corresponding Fourier transforms are $[X(0) \quad X(1) \quad \cdots \quad X(N-1)]$ and $[\tilde{X}(0) \quad \tilde{X}(1) \quad \cdots \quad \tilde{X}(N-1)]$, respectively. If sequence 2 is a circular shift version of sequence 1 by right-shifting the elements to $v$ positions [i.e., $\tilde{x}(n) = x((n-v)_N)$, where $(\cdot)_N$ denotes the modulo operation over period of $N$], then

$$\tilde{X}(k) = X(k)e^{-j(2\pi kv/N)}, \qquad k = 0, 1, \ldots, N-1. \tag{1.67}$$

*Proof:* For any value of $k$, we have

$$\begin{aligned}
\tilde{X}(k) &= \sum_{n=0}^{N-1} \tilde{x}(n)e^{-j(2\pi kn/N)} \\
&= \sum_{n=0}^{N-1} x((n-v)N)e^{-j(2\pi kn/N)} \\
&= \sum_{n=0}^{v-1} x(N-v+n)e^{-j(2\pi kn/N)} + \sum_{n=v}^{v-1} x(n-v)e^{-j(2\pi kn/N)} \\
&= \sum_{n'=N-v}^{N-1} x(n')e^{-j[2\pi k(n'-N+v)]/N} + \sum_{n'=0}^{N-v-1} x(n')e^{-j[2\pi k(n'+v)]/N} \\
&= e^{-j(2\pi kv/N)} \sum_{n=0}^{N-1} x(n)e^{-j(2\pi kn/N)} = X(k)e^{-j(2\pi kv/N)}.
\end{aligned} \tag{1.68}$$

To prove (1.8), let $\boldsymbol{A} = \boldsymbol{\Lambda W}$ and $\tilde{\boldsymbol{H}} = \boldsymbol{W}^H \boldsymbol{A}$. Notice that

$$\boldsymbol{A} = \boldsymbol{\Lambda W} = \frac{1}{\sqrt{N}} \begin{bmatrix} H_0 & H_0 & \cdots & H_0 \\ H_1 & H_1 e^{-j2\pi/N} & \cdots & H_1 e^{-[j2\pi(N-1)]/N} \\ \vdots & \ddots & \ddots & \vdots \\ H_{N-1} & H_{N-1} e^{-j2\pi(N-1)/N} & \cdots & H_{N-1} e^{-[j2\pi(N-1)(N-1)]/N} \end{bmatrix}. \tag{1.69}$$

Using MATLAB notation[‡] we have $\tilde{\boldsymbol{H}}(:, m) = \boldsymbol{W}^H \boldsymbol{A}(:, m)$, and we only need to prove that $\tilde{\boldsymbol{H}}(:, m) = \boldsymbol{H}(:, m)$ for $m = 1, 2, \cdots, N$.

From the definition of $H_k$, $H_k = \sum_{l=0}^{L-1} h_l e^{-j(2\pi kl/N)}$, we have

$$\begin{bmatrix} H_0 \\ H_1 \\ \vdots \\ H_{N-1} \end{bmatrix} = \sqrt{N}\ \boldsymbol{W} \begin{bmatrix} h_0 \\ h_1 \\ \vdots \\ h_{L-1} \\ 0 \\ \vdots \\ 0 \end{bmatrix} = \sqrt{N}\ \boldsymbol{WH}\,(:, 1)\,. \tag{1.70}$$

Thus, $\boldsymbol{A}(:, 1) = \boldsymbol{WH}(:, 1)$ or $\tilde{\boldsymbol{H}}(:, 1) = \boldsymbol{W}^H \boldsymbol{A}(:, 1) = \boldsymbol{W}^H \boldsymbol{WH}(:, 1) = \boldsymbol{H}(:, 1)$. From (1.69) we observe that the $m$th column of $\tilde{\boldsymbol{H}}$ is just the circular shift version of the first column of $\tilde{\boldsymbol{H}}$ by down-shifting the elements $m - 1$ positions. Furthermore, from (1.7), the $m$th column of $\boldsymbol{H}$ is just the circular shift version of the first column of $\boldsymbol{H}$ by down-shifting the elements $m - 1$ positions. Besides, $\tilde{\boldsymbol{H}}(:, 1) = \boldsymbol{H}(:, 1)$. Hence, we conclude that $\tilde{\boldsymbol{H}} = \boldsymbol{H}$.

## REFERENCES

[1] S. B. Weinstein and P. M. Ebert, "Data transmission by frequency division multiplexing using the discrete Fourier transform," *IEEE Trans. Commun. Technology*, vol. COM-19, pp. 628–634, Oct. 1971.

[2] J. A. C. Bingham, "Multicarrier modulation for data transmission: an idea whose time has come," *IEEE Commun. Mag.*, vol. 28, pp. 5–14, May 1990.

[3] "Radio broadcasting systems: digital audio broadcasting to mobile, portable and fixed receivers," *European Telecommunication Standard ETS 300 401*, ETSI, Sophia Antipolis, France, 1995.

[‡]For an arbitrary matrix $\boldsymbol{A}$, the $m$th column of $\boldsymbol{A}$ is denoted by $\boldsymbol{A}(:, m)$. Here, we also count the columns from number 1 onward according to MATLAB.

[4] "Digital video broadcasting (DVB-T): frame structure, channel coding, modulation for digital terrestrial television," *European Telecommunicaton Standard ETS 300 744*, ETSI, Sophia Antipolis, France 1997.

[5] "Part 11: Wireless LAN medium access control (MAC) and physical layer (PHY) specifications, higher-speed physical layer extension in the 5 GHz band," *IEEE802.11a*, 1999.

[6] J. S. Chow, J. C. Tu, and J. M. Cioffi, "A discrete multitone transceiver system for HDSL applications," *IEEE J. Sel. Areas Commun.*, vol. 9, pp. 895–908, Aug. 1991.

[7] Y. G. Li and G. Stüber, *OFDM for Wireless Communications*, Springer, Boston, 2006.

[8] D. Falconer, S. L. Ariyavisitakul, A. Benyamin-Seeyar, and B. Edison, "Frequency domain equalization for single-carrier broadband wireless systems," *IEEE Commun. Mag.*, vol. 40, pp. 58–66, Apr. 2002.

[9] H. Sari and G. Karam, "Orthogonal frequency-division multiple access and its application to CATV networks," *Eur. Trans. Telecommun.*, vol. 9, pp. 507–516, Nov.–Dec. 1998.

[10] "Interaction channel for digital terrestrial television (RCT) incorporating multiple access OFDM," *ETSI DVB RCT*, ETSI, Sophia Antipolis, France, Mar. 2001.

[11] Draft amendament to IEEE standard for local and metropolitan area networks, "Part 16: Air interface for fixed broadband wireless access system–amendament 2: Medium access control modifications and additional physical layer specifications for 2–11 GHz," *IEEE P802.16a/D3-2001*, Mar. 2002.

[12] L. Wei and C. Schlegel, "Synchronization requirements for multi-user OFDM on satellite mobile and two-path Rayleigh fading channels," *IEEE Trans. Commun.*, vol. 43, pp. 887–895, Feb.–Apr. 1995.

[13] S. Barbarossa, M. Pompili, and G. Giannakis, "Channel-independent synchronization of orthogonal frequency division multiple access systems," *IEEE J. Sel. Areas Commun.*, vol. 20, pp. 474–486, Feb. 2002.

[14] Z. Cao, U. Tureli, and Y. D. Yao, "Efficient structure-based carrier frequency offset estimation for interleaved OFDMA uplink," *Proceedings of IEEE ICC 2003*, vol. 5, pp. 3361–3365, May 2003.

[15] U. Sorger, I. D. Broeck, and M. Schnell, "Interleaved FDMA: new spread spectrum multiple-access scheme," *Proceedings of IEEE ICC 1998*, vol. 2, pp. 1013–1017, June 1998.

[16] R. Dinis, D. Falconer, C. T. Lam, and M. Sabbaghian, "A multiple access scheme for the uplink of broadband wireless systems," *Proceedings of IEEE GLOBECOM 2004*, vol. 6, pp. 3808–3812, Nov. 2004.

[17] H. Ekstrom, A. Furusk, J. Karlsson, M. Meyer, S. Parkvall, J. Torsner, and M. Wahlqvist, "Technical solutions for the 3G long-term evolution," *IEEE Commun. Mag.*, vol. 42, pp. 38–45, Mar. 2003.

[18] Y. Ofuj, K. Higuch, and M. Sawahashi, "Frequency domain channel-dependent scheduling employing an adaptive transmission bandwidth for pilot channel in uplink single-carrier-FDMA radio access," *Proceedings of IEEE VTC 2006–Spring*, vol. 1, pp. 334–338 May 2006.

[19] K. L. Baum, T. A. Thomas, F. W. Vook, and V. Nangia, "Cyclic-prefix CDMA: an improved transmission method for broadband DS-CDMA cellular systems," *Proceedings of IEEE WCNC 2002*, vol. 1, pp. 183–188, Mar. 2002.

[20] S. Hara and R. Prasad, "Overview of multicarrier CDMA," *IEEE Commun. Mag.*, vol. 35, pp. 126–133, Dec. 1997.

[21] C. R. Rao and S. K. Mitra, *Generalized Inverse of Matrices and Its Applications*, Wiley, New York, 1971.

[22] S. Haykin, *Adaptive Filtering Theory*, 3rd ed., Prentice Hall, Upper Saddle River, NJ, 1995.

[23] G. H. Golub and C. F. V. Loan, *Matrix Computations*, 3rd ed.; Johns Hopkins University Press, Baltimore, 1996.

[24] X. Wang and H. V. Poor, "Iterative (turbo) soft interference cancellation and decoding for coded CDMA," *IEEE Trans. Commun.*, vol. 47, pp. 1046–1061, July 1999.

[25] Y.-C. Liang, S. Sun, and C. K. Ho, "Block-iterative generalized decision feedback equalizers for large MIMO systems: algorithm design and asymptotic performance analysis," *IEEE Trans. Signal Process.*, vol. 54, pp. 2035–2048, June 2006.

[26] Y.-C. Liang, E. Y. Cheu, L. Bai, and G. Pan, "On the relationship between MMSE-SIC and BI-GDFE receivers for multiple input multiple output channels," *IEEE Trans. Signal Process*, accepted for publication, vol. 56, No. 8, pp. 3627–3637, Aug. 2008.

[27] Y.-C. Liang, Block-iterative GDFE (BI-GDFE) for CP-CDMA and MC-CDMA, *Proceedings of IEEE VTC 2005–Spring*, vol. 5, pp. 3033–3037, June 2005.

[28] Y.-C. Liang, Asymptotic performance of BI-GDFE for large isometric and random precoded systems, *Proceedings of IEEE VTC 2005C–Spring*, vol. 3, pp. 1557–1561, May–June 2005.

[29] L. B. Thiagarajan, S. Attallah, and Y.-C. Liang, "Reconfigurable transceivers for wireless broadband access schemes," *IEEE Wireless Commun. Mag.*, vol. 14, pp. 48–53, June 2007.

[30] C. Y. Wong, R. S. Cheng, K. B. Lataief, and R. D. Murch, "Multiuser OFDM with adaptive subcarrier, bit, and power allocation," *IEEE J. Sel. Areas Commun.*, vol. 17, no. 10, pp. 1747–1758, Oct. 1999.

[31] W. Rhee and J. M. Cioffi, "Increase in capacity of multiuser OFDM system using dynamic subchannel allocation," *Proceedings of IEEE VTC 2000–Spring*, vol. 2, 2000, pp. 1085–1089.

[32] M. Tao, Y.-C. Liang, and F. Zhang, "Resource allocation for delay differentiated traffic in multiuser OFDM systems," *IEEE Trans. Wireless Commun.*, accepted for publication.

[33] D. Kivanc, G. Li, and H. Liu, "Computationally efficient bandwidth allocation and power control for OFDMA," *IEEE Trans. Wireless Commun.*, vol. 2, no. 6, pp. 1150–1158, Nov. 2003.